Thermal evaluation of laminated composite phase change material gypsum board under dynamic conditions

Tongyu Zhou*, Jo Darkwa, Georgios Kokogiannakis

Centre for Sustainable Energy Technologies (CSET), the University of Nottingham Ningbo, 199 Taikang East Road, Ningbo 315100, China

Abstract

Thermal evaluation of non-deform laminated composite phase change material (PCM) gypsum board has been carried out. The theoretical studies covered the analysis of different thicknesses of PCM layers and their corresponding heat transfer rates during energy storage and discharge processes. A simply approach was also provided for determining the appropriate thicknesses of PCM layer under various conditions. For the purpose of experimental study and validation, a laminated gypsum board consisting of a 4 mm PCM layer was evaluated in a naturally ventilated condition. It achieved a maximum heat exchange of 15.6 W/m^2 and a maximum energy storage of 363.7 kJ/m^2. A model room built with the laminated PCM gypsum boards was also evaluated and achieved a maximum temperature reduction of 5 ℃ as compared with 1.8 ℃ for the one with ordinary gypsum board. Even though about 25% of the energy stored could not be released within the targeted period, the overall thermal performance of the PCM gypsum board was quite remarkable. Further heat transfer enhancement mechanism may therefore be necessary for the energy discharge process.

Keywords: Non-deform PCM; Laminated gypsum board; Heat transfer; Energy storage and discharge

1. Introduction

Thermal storage systems for energy conservation in buildings have gained more and more attention. Phase change materials (PCMs) as latent heat storage material are particularly attractive for energy conservation in buildings due to their high energy storage capacity at constant temperature [1-3].

Investigations into composite PCM drywall systems especially gypsum board has drawn high research interests in the past twenty years. Gypsum board is usually found in the interior side of partition walls as a cladding element. This guarantees the use of most of the thermal inertia when PCMs are integrated. Such great potential has therefore led to past efforts towards the development of PCM gypsum board. For instance, Shilei *et al.*[4] immersed a piece of gypsum board in a solution of PCM containing capric acid and lauric acid and achieved energy storage capacity of 39kJ/kg at 24^{o}C. Borreguero *et al.* [5] studied the feasibility of directly embedding

* Corresponding author. Tel.:+86(0) 574 8818 9254
E-mail address: tongyu.zhou@nottingham.edu.cn
Address: 199 Taikang East Road, University park, Ningbo, China

Nomenclature

A Surface area of PCM layer (m^2)
a Constant, defines the temperature varying scope
b Constant, defines the starting temperature
C_p Specific heat (kJ/kg K)
E_a Actual thermal energy storage per unit surface area (kJ/m^2)
E_m Maximum thermal energy storage per unit surface area (kJ/m^2)
e Thickness (m)
e_{pcm} Thickness of PCM layer (m)
H Enthalpy of material (kJ/kg)
H_{ref} Reference Enthalpy (kJ/kg)
Hs Sensible enthalpy (kJ/kg)
ΔH Latent heat (kJ/kg)
h Convective heat transfer coefficient (W/m^2 K)
k Thermal conductivity (W/m K)
L Latent heat capacity of PCM (kJ/kg)
n Steps
q Heat flux (W/m^2)
q_i Heat flux of each step (W/m^2)
T Temperature (K)
T_{init} Initial temperature (K)
T_s Solidus Temperature (K)
T_l Liquidus Temperature (K)
T_{ref} Reference Temperature (K)
T_∞ Air temperature (K)
t Time (s)
V Volume (m^3)

Greek

β Liquid fraction
ρ Density (kg/m^3)
ζ Percentage of energy storage (%)
δ Relative energy storage capacity

microencapsulated PCM in gypsum boards to increase the wall energy storage capacity. It was reported that the composite PCM gypsum boards were able to either increase or reduce the average surface temperature by up to 1.3 ^oC during the heating and cooling processes respectively. Schossig *et al*. [6] numerically and experimentally investigated the thermal performances of PCM gypsum board in a full-size room with external shading device. The test achieved a maximum differential temperature of 2 ℃ between the PCM coated room and the conventional room.

Although significant advances towards the development of PCM gypsum board have been made over the past two decades, there are still integration and heat transfer problems associated with phase change materials. One of the issues is that most of the commercially available microencapsulated PCMs have relatively low thermal conductivities which adversely affect their thermal response after integration into gypsum boards. For these reasons Darkwa and Kim [7] investigated a different integration method by laminating microencapsulated hexadecane PCM onto a gypsum board and then evaluated it against a randomly mixed PCM gypsum board. The results showed that the laminated PCM board was able to release about 27% more latent heat than the randomly mixed type. Further heat transfer enhancement study

was carried out by Darkwa and Zhou [8]. A laminated composite aluminium/hexadecane gypsum board was developed and compared with a pure hexadecane gypsum board sample. The test results revealed faster thermal response by the aluminium/hexadecane sample regarding the rate of heat flux and also achieved about 10% and 15 % heat transfer enhancements during the charging and discharging periods respectively. Its measured effective thermal conductivity also increased by 1.25 W/m ŀK as compared with 0.15 W/m ŀK for pure hexadecane sample. However, relatively lower energy storage density was obtained due to the high porosity of the microencapsulated PCM powder. In order to overcome this problem, Darkwa *et al.* [9] recently developed a novel non-deformed composite hexadecane phase change material based on powder compaction technique. This approach resulted in a PCM tablet with about 97% increase in energy storage density and thermal conductivity value of 2.3 W/m ŀK despite 10% reduction in its latent heat capacity. This study is therefore intended to theoretically and experimentally evaluate the thermal performance of this PCM tablet in a gypsum board.

2. Mathematical modelling and simulation

2.1 Physical model

In actual buildings, gypsum boards are often used on the interior wall areas which are not exposed to the sun, but are coupled to a space-averaged room temperature by convection. To establish an understanding of the thermal performance of an idealized PCM gypsum board, it is assumed that the board has only one surface experiencing convective heat transfer with the surrounding air. Fig. 1 shows a diagram of a laminated composite PCM gypsum board consisting of a gypsum board and a PCM layer made up of PCM tablets.

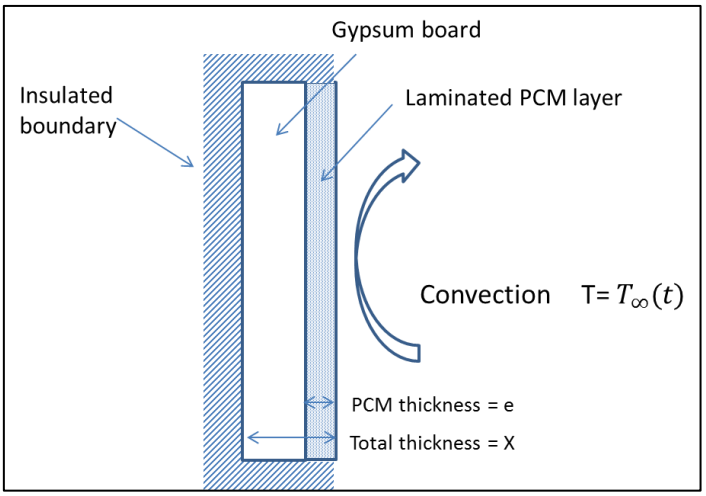

Figure 1: Laminated PCM gypsum board

2.2 Governing equations

The assumptions for the modelling are summarized as follows:

- The heat transfer in PCM board is dominated by one-dimensional conduction.
- The heat transfer between PCM and air is by convection only.
- Both the liquid and solid phases of PCM are isotropic and homogeneous, thus their thermophysical properties are taken to be constants at each phase.
- Thermal energy stored by gypsum board is neglected as it is significantly smaller as compared with the energy stored by means of latent heat in PCM.

An enthalpy porosity technique [10] was used in this study for modelling the solidification/melting process. Accordingly, the general governing equation of one-dimensional heat transfer in PCM is given as:

$$\frac{\partial}{\partial x}\left(k\frac{\partial T}{\partial x}\right) = \rho\frac{\partial H}{\partial t} \tag{1}$$

Where, the enthalpy of the material (H) was computed as the sum of the sensible enthalpy (H_s), and the latent heat (ΔH) as presented in Eq. 2:

$$H = H_s + \Delta H \tag{2}$$

Where the sensible enthalpy is given as:

$$\mathrm{H}_s = H_{ref} + \int_{T_{ref}}^{T} C_p dT \tag{3}$$

The latent heat content (ΔH) is written as:

$$\Delta H = \beta L \tag{4}$$

L is the latent heat capacity of the PCM, and β is the liquid fraction during the phase change which occurs over a range of temperatures $T_s < T < T_l$, defined by the follow relations:

$$\beta = \begin{cases} 0 & (T < T_s) \\ \frac{T-T_s}{T_l-T_s} & (T_s \le T \le T_l) \\ 1 & (T > T_l) \end{cases} \tag{5}$$

Where, T_s and T_l are the solidus and liquidus temperature of PCM, respectively.

2.3 Initial and boundary conditions

At time $t = 0$, the whole PCM layer was taken to be solid that was maintained at a temperature T_{init} below the solidus temperature T_s of the PCM. The initial condition at $t = 0$ in the model is therefore given by:

$$T(x,t) = T_{init} \qquad (0 \le x \le e,\ t = 0) \tag{6}$$

Where, e is the thickness of PCM layer.

According to the assumption, one surface of PCM layer experiences convective heat transfer with the surrounding air, the other surface is adiabatic. The boundary condition is therefore given by:

$$\begin{cases} \frac{\partial T}{\partial x} = 0 & (x = 0) \\ k\frac{\partial T}{\partial x} = h\big(T(x,t) - T_\infty(t)\big) & (x = e) \end{cases} \quad (7)$$

Where, $T_\infty(t)$ is the air temperature. To model the PCM under dynamic boundary conditions, it was assumed that $T_\infty(t)$ varies sinusoidally with time *t (s)*. It represents the diurnal indoor temperature fluctuation. The equation for $T_\infty(t)$ is given by:

$$T_\infty(t) = a \cdot \sin\left(2\pi \cdot \frac{t-21600}{86400}\right) + b \quad (8)$$

Where the constant "*a*" defines the temperature varying scope; and the constant "*b*" defines the starting temperature.

2.4 Simulation

In this study, the grid of the physical model was built using the Gambit software and the numerical solution was obtained using Fluent 6.3 software. The effects of the time step and grid size on the solution were carefully examined. The grid sizes of 0.1, 0.2 and 0.5 mm and three different time steps, i.e. 10, 100 and 1000 s were checked. As appears from Fig.2, the results obtained for surface temperature variation of PCM gypsum board were independent of the grid size. Fig.3 shows the results for three different time steps. One can see that there is no difference between time steps 10s and 100s, but a deviation with time step of 1000s. These indicate that the results obtained were independent of all above grid sizes and time steps of 10 and 100s. Therefore in order to save computational resources and calculation time as well as minimising errors, a grid size of 0.2 mm and time step of 100 s were used. Convergence of the solution was checked at each time step for a convergence criterion of 10^{-6} for the energy equation.

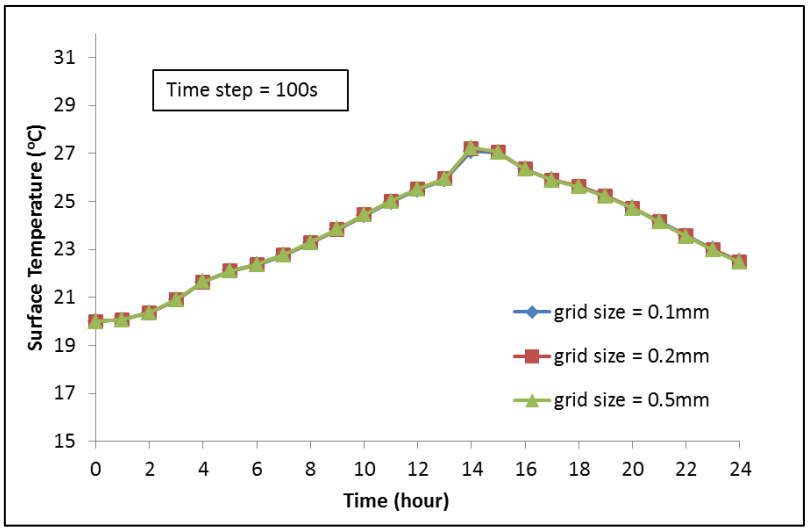

Figure 2: Grid dependency of the numerical solution.

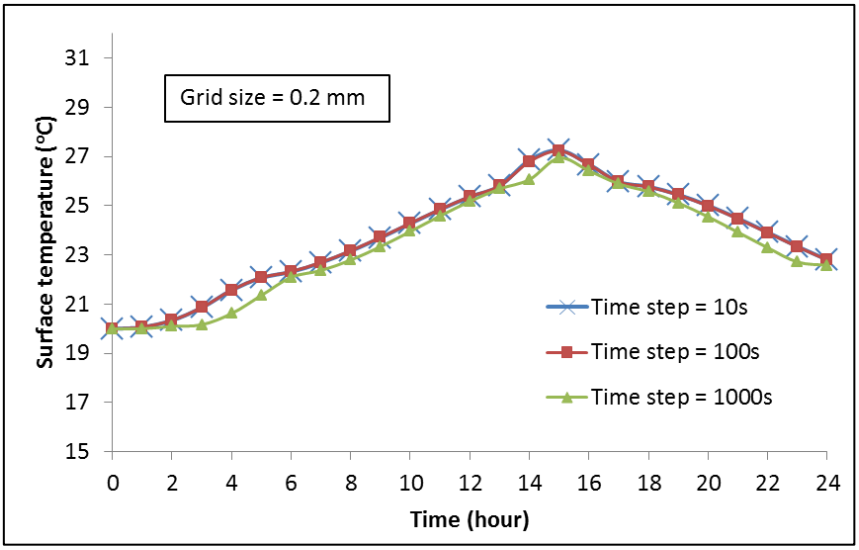

Figure 3: Time dependency of the numerical solution.

The evaluation of thermal performance of PCM gypsum board was conducted under air temperature variations of 20~28 ℃ corresponding to condition in most naturally and forced ventilated room (convective heat transfer coefficients h = 5, 10 and 15 W/m^2 K). It was then simulated over a period of 24 hours for its thermal performance based on data in Tab. 1.

Table 1: The simulation data

Items	**PCM gypsum board ***	
Components	PCM layer	gypsum
Density (kg/m^3)	821	950
Specific heat (kJ/kg K)	2.20	0.84
Latent heat (kJ/kg)	111.80	-
Phase change temperature range (℃)	22 ~ 26	-
Thermal conductivity (W/m k)	2.30	0.16
Thickness (mm)	e=2,4,6,8,10	10,8,6,4,2
Total thickness X (mm)	12	
Air temperature variation (℃)	20~28	
Heat transfer coefficient (W/m^2 K)	5,10,15	

*Data source: Darkwa *et al.* [9]

2.5 Results and analysis

As shown in Fig.4, there was significant temperature difference between the surface of PCM gypsum board and the surrounding air. The 2 mm PCM layer responded faster than the other layers and reached the maximum surface temperature of about 28 ℃ at 13.5 hours. There was a time lag of about 3.5 hours for the 4 mm layer and about 4-5 hours for the 6, 8 and 10 mm layers. These conditions are demonstrated

with the contours of static temperature in Fig. 5 where the 2 mm layer was fully melted after the air had reached its peak temperature. The temperature differences also resulted in various heat exchange rates as shown in Fig. 6. The 6, 8 and 10 mm layers of PCM achieved relatively higher heat flux rates than the 2 mm and 4 mm layers due to the larger temperature differences between PCM and air for the 6, 8 and 10 mm layers.

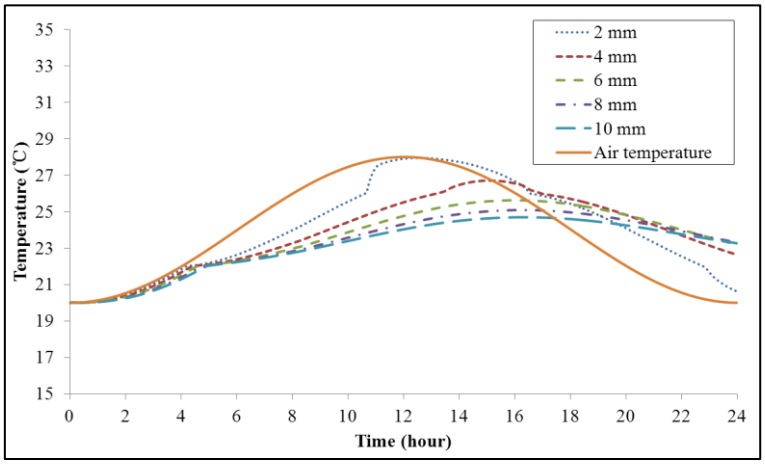

Figure 4: Surface temperature profiles for h = 5 W/m^2 K

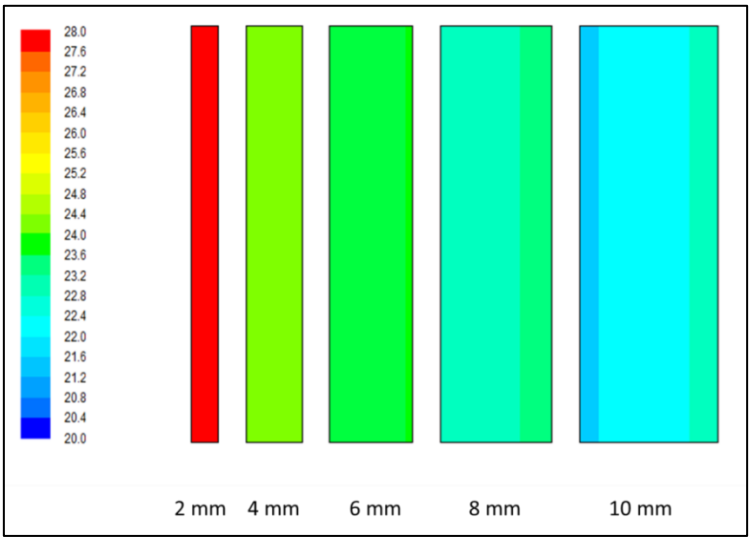

Figure 5: Contours of static temperature of PCM layers after peak air temperature for h = 5 W/m^2 K

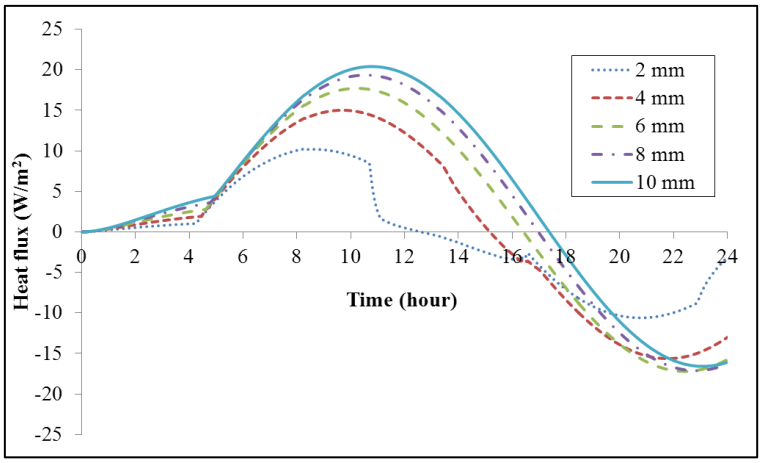

Figure 6: Heat flux profiles for h = 5 W/m^2 K

Fig. 7 shows the surface temperature profiles for different thicknesses for h = 10 W/m^2 K. There was very small time lag between the peak air temperature and the 2 and 4 mm thick PCM layers thus making them more thermally responsive than the others. There was a time lag of 1 hour for the 6 mm, 3 hours for the 8 mm and 4 hours for the 10 mm layers. The temperature contours in Fig. 8 shows that the 2 mm and 4 mm layers were fully melted after the peak air temperature was reached when compared with other layers. The corresponding heat flux profiles for the layers are shown in Fig. 9. In comparison with h = 5 W/m^2 K there was some level of increase in heat flux rates for all the thicknesses except the 2 mm thick layer which remained unchanged. The increase in heat flux rate for the 4 ~ 10 mm layers was approximately between 25 % and 50 %.

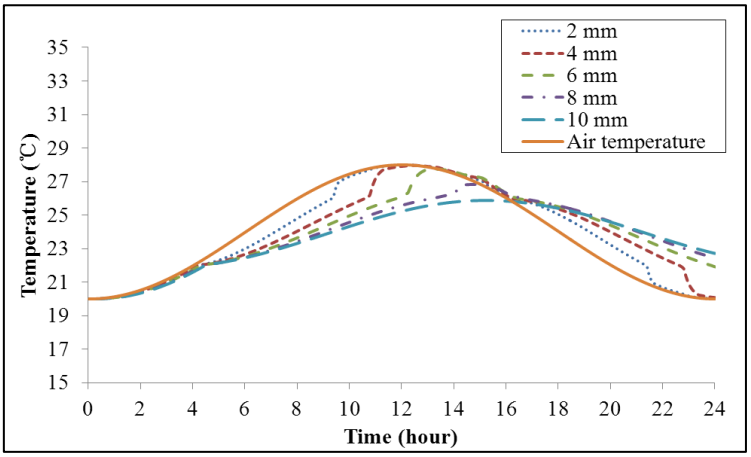

Figure 7: Surface temperature profiles for h = 10 W/m^2 K

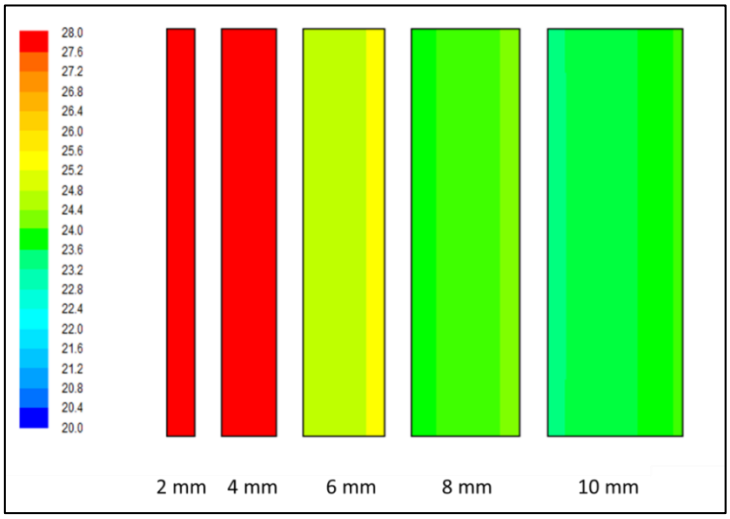

Figure 8: Contours of static temperature of PCM layers after peak air temperature for h = 10 W/m^2 K

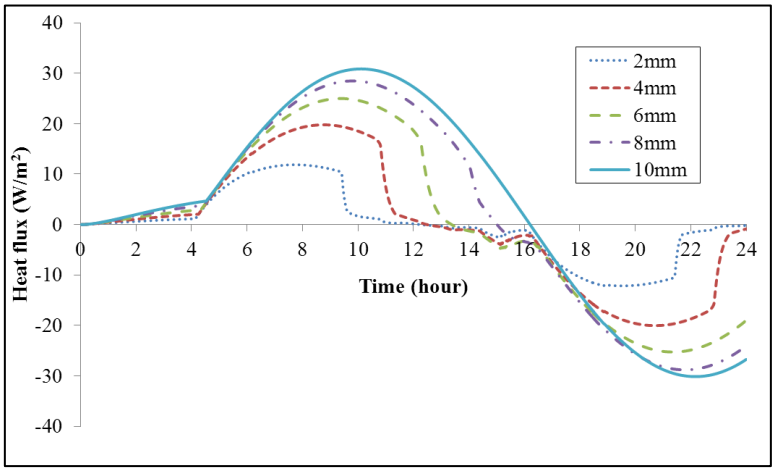

Figure 9: Heat flux profiles for h = 10 W/m^2 K

Fig. 10 illustrates the surface temperature profiles for h = 15 W/m^2 K and shows that the time lag affected only the 8 mm and 10 mm layers. The 2mm, 4 mm and the 6 mm layers were fully melted before the peak air temperature was reached. These are supported with the contours of static air temperatures in Fig. 11. There was a slight improvement in the heat flux rates as shown in Fig. 12 despite higher value of convective heat transfer coefficient. The maximum heat flux achieved was about 37.5 W/m^2 as compared with 30.2 W/m^2 obtained under h = 10 W/m^2 K.

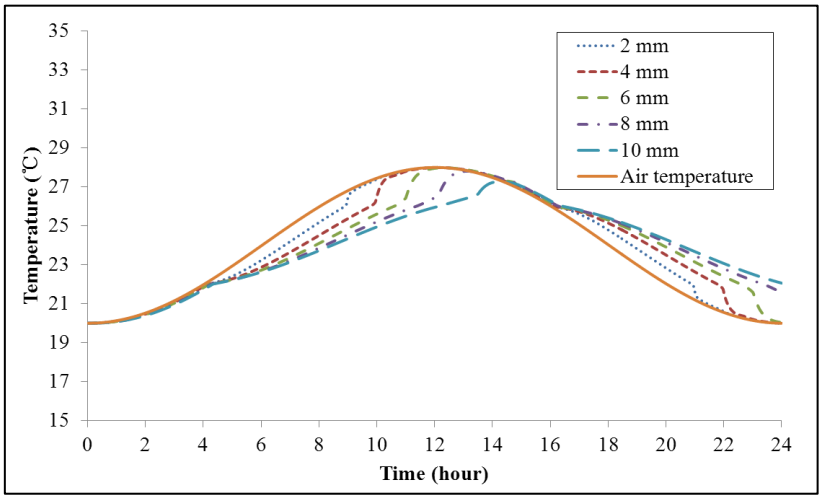

Figure 10: Surface temperature profiles for h = 15 W/m^2 K

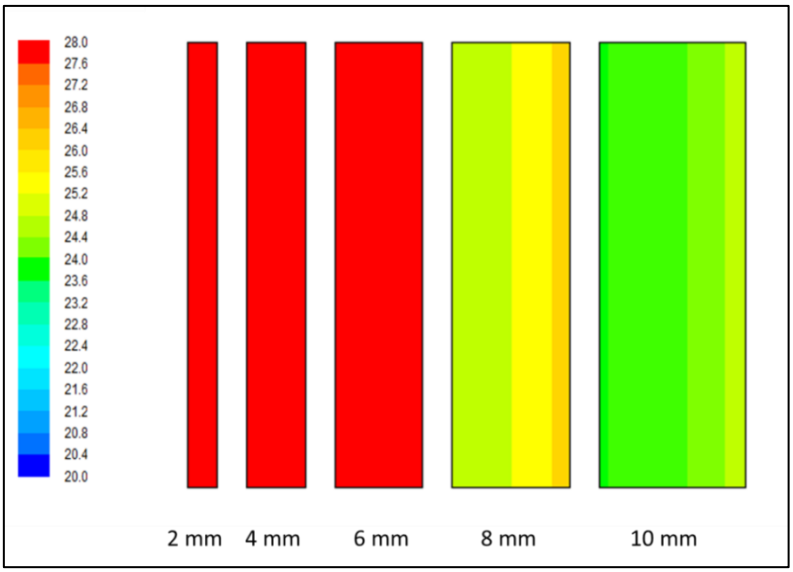

Figure 11: contours of static temperature of PCM layers after peak air temperature for h = 15 W/m^2 K

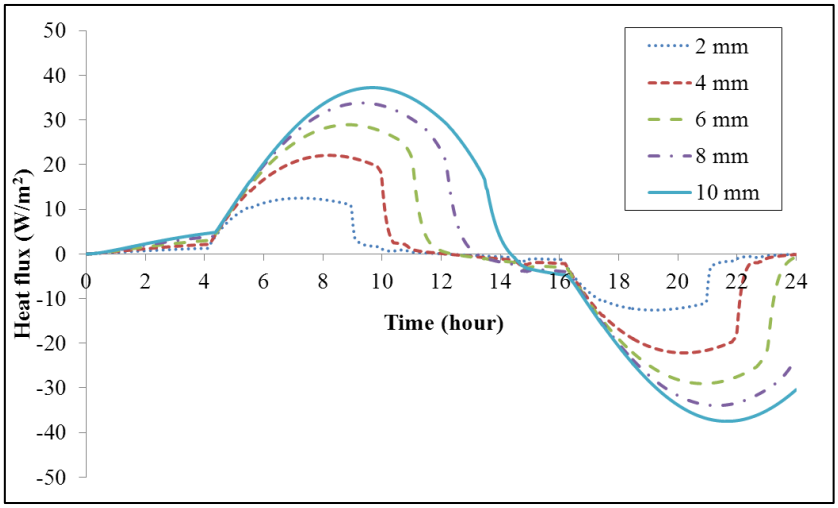

Figure 12: Heat flux profiles for h = 15 W/m^2 K

2.6 Selection of thicknesses of PCM layer

The selection of the appropriate thickness of PCM layer depends on room temperature variation and heat transfer coefficient between the PCM and the surrounding air. It also depends on an indicator called percentage of energy storage (ζ). It is defined as the ratio of the actual thermal energy (E_a) stored by the PCM to its maximum heat storage capacity (E_m) as expressed in Eq. 9 [11].

$$\zeta = \frac{E_a}{E_m} \times 100\% \tag{9}$$

Where the actual energy stored by PCM (kJ/m^2) is expressed as:

$$E_a = \sum_n q_i \cdot t \tag{10}$$

The maximum heat storage capacity per unit surface area (kJ/m^2), which is made up of both latent heat and sensible heat, is also expressed as:

$$E_m = \frac{\rho \cdot V \cdot L + \int_{T_min}^{T_max} \rho \cdot V \cdot C_p \cdot dT}{A} = \rho \cdot e_{pcm} \cdot L + \int_{T_{min}}^{T_{max}} \rho \cdot e_{pcm} \cdot C_p \cdot dT \tag{11}$$

For the selection of the most appropriate thickness, two conditions need to be satisfied: large energy storage capacity and high percentage of energy storage. Now, using Eqs. 10 and 11, actual energy storage capacities and the corresponding percentages of energy storage can be summarised as shown in Tab. 2 and plotted in Figs. 13 ~ 15. The points of intersections in the graphs indicate the appropriate thicknesses as: approximately 4 mm for h = 5 W/m^2 K, 8 mm for h = 10 W/m^2 K and about 10 mm for h = 15 W/m^2 K. It should be noted that the appropriate thicknesses were selected amongst five predetermined thicknesses in the simulation data, i.e. 2, 4, 6, 8 and 10 mm.

For the benefit of the experimental study and validation, a 4 mm thickness of PCM layer was selected for the condition of h = 5 W/m^2 K which satisfies most naturally ventilated rooms.

Table 2: Actual energy storage capacities and percentages of PCM layers of different thicknesses

PCM layer (mm)	**Actual energy storage capacity (E_a) kJ/m^2**			**Energy storage percentage (ζ) %**		
	h=5 W/m^{2}K	h=10 W/m^{2}K	h=15 W/m^{2}K	h=5 W/m^{2}K	h=10 W/m^{2}K	h=15 W/m^{2}K
2	196.3	196.7	196.7	99.1	99.3	99.3
4	391.7	392.9	393.3	98.9	99.2	99.3
6	473.5	582.8	587.0	79.7	98.1	98.8
8	484.8	770.7	775.5	61.2	97.3	97.9
10	487.2	832.8	965.4	49.2	84.1	97.5

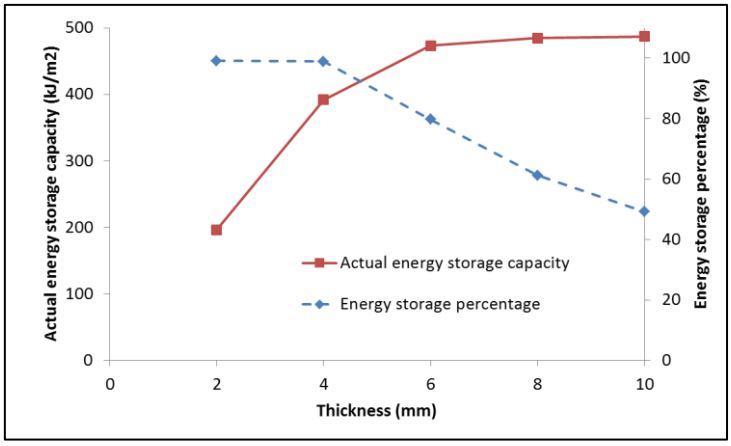

Figure 13: Actual energy storage capacity against energy storage percentage for h = 5 W/m^2 K

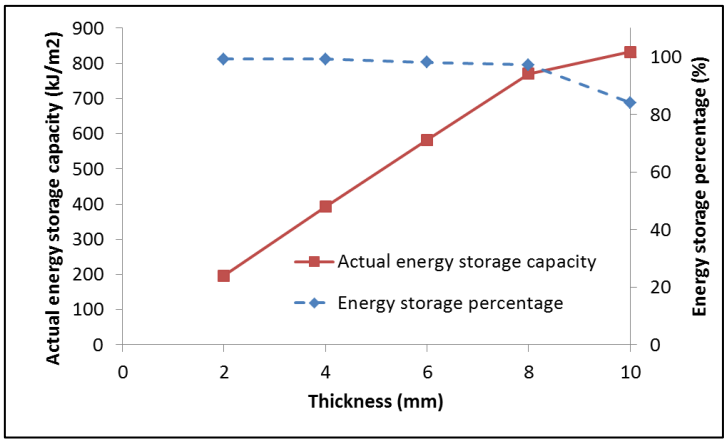

Figure 14: Actual energy storage capacity against energy storage percentage for h = 10 W/m^2 K

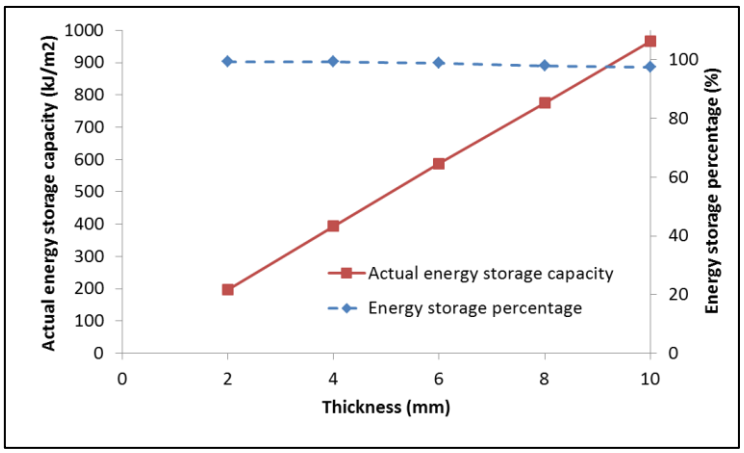

Figure 15: Actual energy storage capacity against energy storage percentage for h = 15 W/m^2 K

3. Experimental evaluation

3.1 Sample preparation

A number of composite PCM rectangular tablets, each measuring 30 mm * 30 mm * 4 mm as shown in Fig.16 were prepared based on previous work and specifications given in Tab. 1 by Darkwa *et.al.* [9]. The tablets were then laminated with PVA adhesive material onto a gypsum board which measured 500 mm * 300 mm * 8 mm thick. The final test sample was therefore made up of a laminated 4mm PCM layer and 8 mm gypsum board.

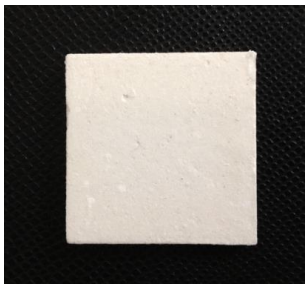

Figure 16: Picture of PCM tablet

3.2 Sample testing

The test was carried out in a climate controlled chamber (Fig. 17) which had an operational temperature range of - 20^{o}C to 80 ^{o}C for a relative humidity ranging from 30% to 95%. The air temperatures and heat flux were respectively measured with a set of calibrated thermocouples (Omega K-type thermocouple TT-K-30-SLE, ±1.1 ^{o}C) and thin film heat flux sensors (Omega HFS-04, ±0.5 W/m^{2}) through a data logger (Agilent 34970A + 20 channel multiplexer 34901A) and a dedicated computer. In order to achieve a uniform air around the test sample a 1m * 1m * 1m wooden box (Fig. 18) was built and placed around it as displayed in Fig. 19. This prevented the forced air flow from the chamber's fan to affect the sample and any air flows around the sample were only occurring mainly due to natural buoyancy. An approximate sinusoidal variation (20 ~ 28 ℃) of the air temperature was then prescribed to simulate a daily indoor temperature variation which corresponds to the same condition in the numerical study.

3.2.1 Test procedure

The thermal performance test was carried out over a 24-hr full-cycle condition covering both heating and cooling processes and repeated for five times but on every other day. The average values of measurements were then used for analysing. The specific procedures are as follows.

(a) The chamber was initially cooled down until the surface temperature of the sample reached 20 ^{o}C.

(b) The chamber was then switched on to the heating mode and was programmed to

heat the air in the wooden box slowly from 20 ^{o}C to 28 ^{o}C over a 12-hour period.

(c) After achieving the desired temperature, the heating process was terminated to allow the cooling process to begin. Similarly, the cooling process was controlled within a 12- hour period whilst the temperatures were monitored from 28 ^{o}C to 20 ^{o}C.

Figure 17: Climate controlled chamber

Figure 18: Picture of the wooden box in the chamber

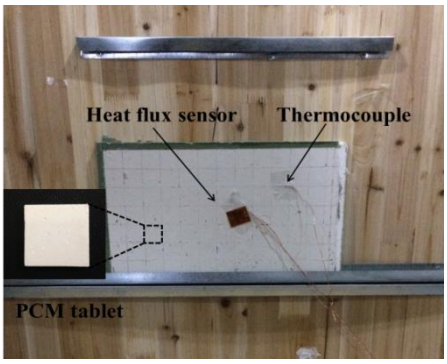

Figure 19: Arrangement of test sample and accessories inside the wooden box

3.2.2 Test results

The average test results from the five 24-hr measurements are used for the discussion below. The estimated deviation from the average values of the measurements was about ± 0.3 ℃ on temperature measurements and ± 0.5 W/m^2 on heat flux due to potential errors of instruments and experimental conditions. Fig. 20 shows the theoretical and experimental surface temperature profiles of the sample during energy storage and release periods. During the initial stage, both profiles displayed similar trends until phase change process begun. The profiles show theoretical/experimental time lag of 3.3/3.5 hours between the peak surface temperature of the board and the peak space temperature. There was also a differential temperature of up to 2 ℃ between the two sets of results at the end of the discharge process but found them to be fairly comparable.

The thermal effectiveness of the PCM gypsum board was also evaluated by measuring the heat flux data and using it to calculate the cumulative energy storage/discharge. As

shown in Fig. 21, the theoretical/experimental heat flux profiles were found to be fairly close with peak values of 15.2/15.6 W/m^2 during the charging process and 14.8/11.75 W/m^2 for the discharge mode. The corresponding cumulative energy storage/discharge profiles are also shown in Fig. 22. The theoretical energy storage was obtained as 391.7kJ/m^2 as against an experimental value of 363.7kJ/m^2. During the discharge mode, the theoretical and experimental energy discharges were achieved as 301kJ/m^2 and 272.7kJ/m^2 respectively. It should also be noticed that the experimental energy storage percentage reached a fairly high value of 91.8% even though it was still about 7.1% lower than numerical value of 98.9%. It indicates that 4 mm was an appropriate thickness of PCM layer that guaranteed both high energy storage capacity and high storge precentage under this condition. It also shows that there was however a small amount of PCM not melted at this stage (the energy storage would at least be about 381.6 kJ/m^2 if PCM was fully melted, corresponding to its potential latent and sensible heat storage capacity). In general, the numerical and experimental results were found to be in good agreement, i.e. approximately 6% difference in time lag, 3% and 21% in peak values of heat flux in charging and discharging processes respectively, 7% and 9% in cumulative energy storage and discharge capacity respectively. However analysis of the results shows that about 25 % of the energy stored could not be released within the monitored period of 24 hrs.

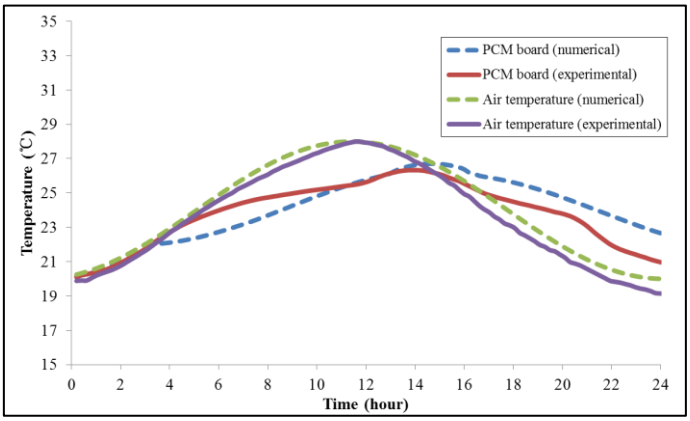

Figure 20: Surface temperature profile of PCM gypsum board

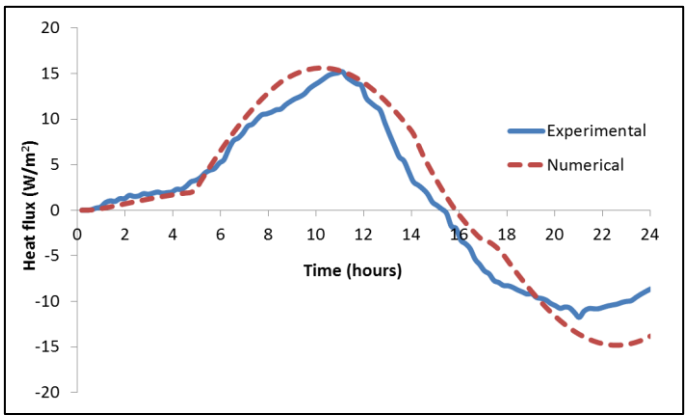

Figure 21: Heat flux profile of PCM board

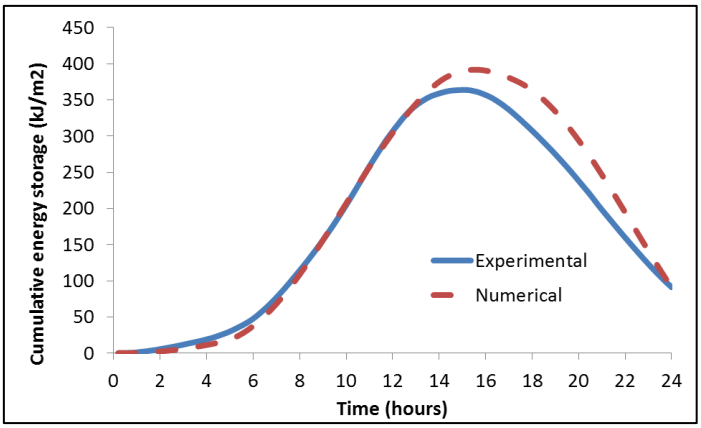

Figure 22: Cumulative energy storage and release profiles of PCM board

3.3 Thermal evaluation of PCM gypsum board in model rooms

In order to evaluate the thermal effectiveness of the developed sample, two identical model rooms (one with gypsum boards and the other with PCM gypsum boards) were built and tested in the climate chamber. The full and exploded views of the rooms are shown in Figs. 23 and 24 respectively. Due to space limitation, their sizes were scaled down to 0.5m * 0.5 m * 0.3 m. The external surfaces of the wall board and roof were all insulated with 20 mm polyurethane foam except the front elevation wall which was considered as a heat entrance to the model room. For this reason the PCM model room had three of its internal walls fully laminated with PCM layers as shown in Fig. 24.

The same procedure as described in Section 3.2.1 was then adopted for this test. However an external sinusoidal temperature variation between 20~30 ℃ was used in order to characterize the decrement factor due to the PCM layer.

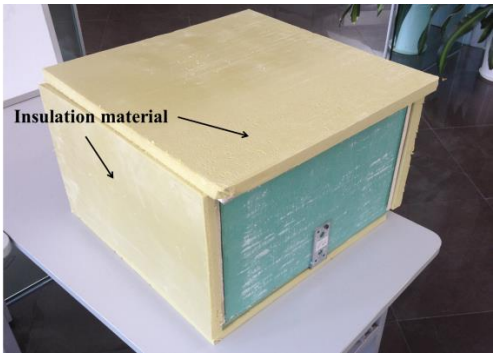

Figure 23: Model room

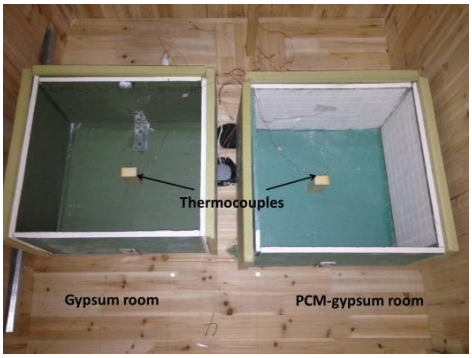

Figure 24: Exploded views of the rooms

3.3.1 Results and analysis

Fig. 25 shows the air temperature profiles inside the two model rooms during heating and cooling processes. It can be seen that the gypsum room displayed much steeper

temperature gradient than the PCM-gypsum room. The temperature in the gypsum room also reached a state of equilibrium with the external air at 17 hours whereas the PCM-gypsum room reached its equilibrium condition much later at 20 hours i.e. 8 hours after the peak external air temperature. The overall test analysis shows that the PCM-gypsum room was able to achieve a maximum temperature reduction of 5 ℃ between external and internal environment as compared with 1.8 ℃ for the gypsum room.

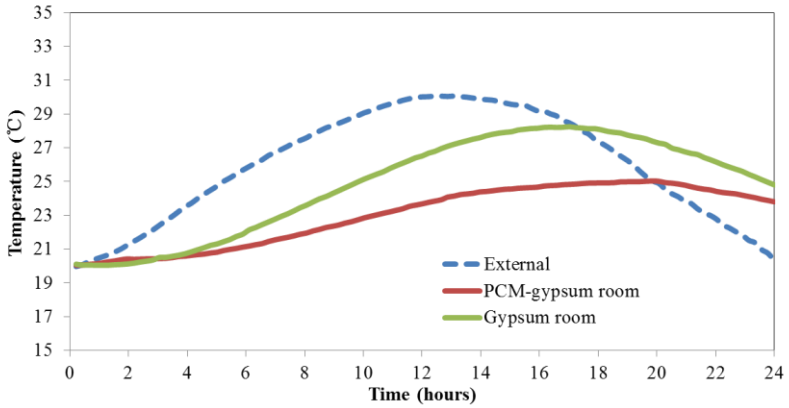

Figure 25: Mean air temperature profiles in model rooms

4. Conclusions

The study did focus on the theoretical and experimental evaluation of a non-deform laminated PCM gypsum board. Based on the theoretical studies, different thicknesses of PCM layers and heat transfer coefficients were analysed for their thermal responsiveness. According to the results, the appropriate thicknesses of PCM layer under different convective heat transfer coefficients were selected as follows: approximately 4 mm for h = 5 W/m^2 K, 8 mm for h = 10 W/m^2 K and about 10 mm for h = 15 W/m^2 K.

For the benefit of the experimental study and validation, a 4 mm thickness of PCM layer was laminated onto a gypsum board and evaluated in a naturally ventilated controlled chamber. Its corresponding theoretical and experimental cumulative energy storage/discharge values were also determined and found to be in a good agreement. In order to evaluate its thermal effectiveness the PCM gypsum board was incorporated into a model room and evaluated against an ordinary gypsum board room under the same environmental condition.

Analysis of the results showed a significant display of temperature moderation by the PCM gypsum room thus confirming its effectiveness as an energy storage material for building application. The specific findings may therefore be summarised as follows:

- Theoretical/experimental peak heat flux values of the PCM board were obtained as 15.2 / 15.6 W/m^2 and 14.8 / 11.75 W/m^2 for the charging and discharging processes respectively.

- Theoretical maximum energy storage/discharge was obtained as 391.7 kJ/m^2 / 301 kJ/m^2 as against 363.7 kJ/m^2 / 272.7 kJ/m^2 for the experimental process.
- The PCM gypsum room achieved a maximum temperature reduction of 5 ℃ in comparison with 1.8 ℃ for the gypsum room.

Even though about 25% of the energy stored could not be released within the monitored period, the overall performance was considered to be satisfactory. However, some form of heat transfer enhancement during the discharge process is considered as necessary. The theoretical study could be expanded in the future with the development of PCM models within whole building simulation programs in order to be able to theoretically evaluate the integration of non-deform laminated PCM gypsum boards together with the rest of the building components. The experimental evaluation could also be carried out in the future with full scale samples under different climate and indoor conditions.

Acknowledgement

The authors wish to thank the Ningbo Science and Technology Bureau, China for supporting this research under the Key Laboratory of Integrated Thermal Energy Storage Technologies (ITEST) for buildings project.

References

[1] L. Pérez-Lombard, J. Ortiz, C. Pout, A review on buildings energy consumption information, Energy and Buildings, 40 (2008) 394-398.

[2] X. Wang, Y.P. Zhang, W. Xiao, R.L. Zeng, Q.L. Zhang, H.F. Di, Review on thermal performance of phase change energy storage building envelope, Chinese Science Bulletin, 54 (2009) 920-928.

[3] V.V. Tyagi, S.C. Kaushik, S.K. Tyagi, T. Akiyama, Development of phase change materials based microencapsulated technology for buildings: A review, Renewable and Sustainable Energy Reviews, 15 (2011) 1373-1391.

[4] S. Lv, G. Feng, N. Zhu, L. Dongyan, Experimental study and evaluation of latent heat storage in phase change materials wallboards, Energy and Buildings, 39 (2007) 1088-1091.

[5] A.M. Borreguero, M. Carmona, M.L. Sanchez, J.L. Valverde, J.F. Rodriguez, Improvement of the thermal behaviour of gypsum blocks by the incorporation of microcapsules containing PCMS obtained by suspension polymerization with an optimal core/coating mass ratio, Applied Thermal Engineering, 30 (2010) 1164-1169.

[6] P. Schossig, H.M. Henning, S. Gschwander, T. Haussmann, Micro-encapsulated phase-change materials integrated into construction materials, Solar Energy Materials and Solar Cells, 89 (2005) 297-306.

[7] K. Darkwa, J.S. Kim, Dynamics of energy storage in phase change drywall systems, International Journal of Energy Research, 29 (2005) 335-343.

[8] J. Darkwa, T. Zhou, Enhanced laminated composite phase change material for energy storage,

Energy Conversion and Management, 52 (2011) 810-815.
[9] J. Darkwa, O. Su, T. Zhou, Development of non-deform micro-encapsulated phase change energy storage tablets, Applied Energy, 98 (2012) 441-447.
[10] Fluent 6.3 User's Guide, in, Fluent Inc., 2006.
[11] G. Evola, L. Marletta, F. Sicurella, A methodology for investigating the effectiveness of PCM wallboards for summer thermal comfort in buildings, Building and Environment, 59 (2013) 517-527.